Materials Research, Vol. 5, No. 3, 315-320, 2002.

Synthesis and Characterization of the TAPO-5 Molecular Sieve

Sarah P.O. Rios, Ricardo Pereira and Dilson Cardoso*

Universidade Federal de São Carlos,
Programa de Pós-Graduação em Engenharia Química - Laboratório de Catálise
Rodovia Washington Luís, Km 235, C.P. 676, 13565-905 São Carlos - SP, Brazil

Received: September 27, 2001; Revised: July 10, 2002

Aluminophosphate sieves with AFI structure substituted by Ti (denominated TAPO-5) have been synthesized hydrothermally. These materials were characterized by X-ray diffraction (XRD), chemical analysis (ICP), scanning electronic microscopy (SEM), ultraviolet diffuse reflectance spectroscopy (DRS-UV) and thermogravimetric analysis (TGA). XRD results showed the materials have good TAPO-5 crystallinity, although DRS-UV spectra indicated anatase phase as contamination. TGA analysis showed mass loss in the range of high temperatures, which can be attributed to protonated template decomposition. This indicates the existence of structural charge as a consequence of Ti incorporation into AFI structure

Keywords: *molecular sieves, AFI, TAPO-5, titanium aluminophosphates, synthesis*

1. Introduction

Zeolites or zeotypes became very important materials in catalysis since their capacity to separate substances according to size and shape was observed. The structures of these materials are very varied and in general, they are the same for aluminophosphates and aluminosilicates (zeolites). However, there are some structures that exist for aluminophosphates and derivates, but do not for zeolites, as the case for the AFI structure (Fig. 1). This structure is constituted by the union of the six members rings with the four members rings and is too easy to obtain as aluminophosphate, but very hard to synthesize as silicate[1] (zeolite SSZ-24).

The aluminophosphates are formed by intercalation of $[AlO_4^-]$ and $[PO_4^+]$ tetrahedral and don't have net charge in their structures. The isomorphous substitution of these tetrahedral for an other, like $[MgO_4^{-2}]$ or $[TiO_4]$, can create an negative charge in the framework and change drastically the properties of the material (Fig. 2).

When investigators of Enichem industry synthesized TS-1, a molecular sieve containing titanium in its MFI structure[2], and identified its catalytic advantages in heterogeneous oxidation, there was an increase in the research for other molecular sieves containing transition metals in their structure. So, the interest in synthesizing titanium-aluminophosphate arose by the fact that they can be used in heterogeneous oxidations and have some different properties compared to TS-1, namely, higher microporous diameter and hydrophilicity.

The incorporation of titanium in the AFI aluminophosphate forms TAPO-5 and the synthesis of this material involves generally the use of Ti organic sources[3-8]. As these compounds hydrolyse very easily, sometimes the TAPOs have TiO_2 anatase as contaminant phase. Zahedi-Niaki et al. synthesized TAPO-5 with different Ti contents, but the incorporation of this element in the solid was very low[9].

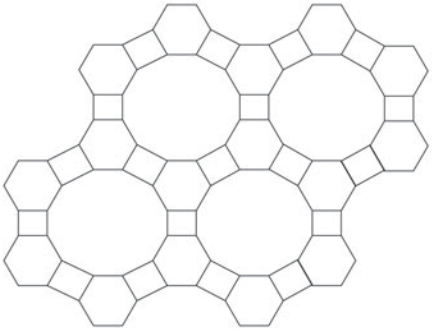

Figure 1. The AFI structure.

---

*e-mail: dilson@power.ufscar.br

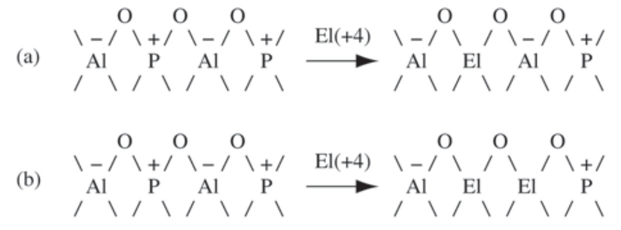

Figure 2. Isomorphous substitution on an AlPO structure: a) $[PO_4^+]$ by $[ElO_4]$ and b) both $[PO_4^+]$ and $[AlO_4^-]$ by $2[ElO_4]$.

In order to avoid the use of the unstable Ti organic sources, the present work verifies the possibility of using hexafluorotitanic acid as Ti source for the synthesis of TAPO-5, as well the possibility of incorporating different Ti contents in the AFI structure.

2. Experimental Procedure

Synthesis

Titanium-aluminophosphate samples were synthesized hydrothermally under autogenous pressure, with $x TiO_2:(1-x/2)Al_2O_3:P_2O_5:TEA:100H_2O:6xHF$ as molar composition of the synthesis reaction mixture, where $x = 0$; 0.01; 0.03; 0.06 e 0.1. The H_2TiF_6 solution (5% w/w) was prepared from the reaction between HF (Carlo Erba, 50%) and TiO_2 (Degussa Hülls). The Al_2O_3 source was pseudoboehmite (Condea) and that of P_2O_5 was phosphoric acid (Carlo Erba, 85%) and TEA is the triethylamine (Carlo Erba, 99.5%) used as AFI structure template. The autoclaves containing the reaction mixtures were submitted to 170 °C and removed in different crystallization times ($t_c = 4$; 8; 22; 28 and 46 h). The solids were centrifuged and washed several times, dried at 110 °C and codified (TixTy, where x indicates the Ti contents, Ty = crystallization time. For the samples which code has no information about the crystallization time, means that Ty = 46 h). The crystallinity was determined by the sum of the peaks areas at around $2\theta = 14.8$; 19.7; 21.0 and 22.0°.

In a typical gel preparation, using $x = 0.03$, 10.73 g of pseudoboehmite were dispersed in 32 ml of deionized water and stirred overnight. Then, 9.5 ml of the phosphoric acid diluted in 72 ml of water was added to the dispersed pseudoboehmite and maintained under stirring during 1 h. Subsequently, 9.7 ml of TEA were added to the mixture, and finally, after stirring during 0.5 h, 1.8 ml of 5% w/w H_2TiF_6 solution diluted in 10 ml of water were added and stirred for more 0.5 h. The final mixture was equally divided in five 70 ml autoclaves and crystallized at 170 °C as already specified. The samples code is indicated in the Table 1.

Characterization

The samples were analyzed by powder X-ray diffraction (XRD, Rigaku-GeigerFLEX) in a scan range of 2θ between 3 and 40° using a scan speed of 2 °/min and Cu-Kα as X-ray source.

Ti, Al and P contents were measured by chemical analysis through ICP methods (Thermo Jarrel Ash), dissolving 0.1 g of the solids in 4 ml HCl (Mallinckrodt, 37%) and 2 ml HNO_3 (Mallinckrodt, 65.5%) mixture. The solution was finally diluted in a 100 ml volumetric flask.

The micrographs of the samples were obtained from scanning electron microscopy (Zeiss, model DSM-940-A). For this purpose, some drops of the sample dispersed in acetone were placed in a sample holder, dried and coated with gold.

Diffuse reflectance spectra in the UV region were recorded from a Varian Cary 5 UV-Vis-NIR spectrophotometer and plotted using Schuster-Kubelka-Munk function (SKM)[10] against $BaSO_4$ as reference. The SKM equation is:

$$F(R_\infty) = (1- R_\infty)^2/2R_\infty \qquad (1)$$

where, R_∞ is the relation between the light intensity reflected from the sample and the light intensity reflected from the reference. This equation is more adequate for quantitative analysis of spectra obtained by diffuse reflectance than the Lambert-Beer equation.

Thermogravimetric analysis (SDT 2980 Simultaneous DSC-TGA) was done in oxidant as well inert ambient with a gas flux of 100 ml.min^{-1} air and 30 ml.min^{-1} of nitrogen.

Table 1. Chemical analysis of TAPO-5 containing different Ti contents synthesized with 46 h.

Sample	x	X_{gel}	X_s	Y_s	Z_s	$[(P+Ti)/Al]_s$	$[(P+Ti)/(Al+Ti)]_s$
Ti1	0.01	0.0025	0.004	0.487	0.509	1.0534	1.0448
Ti3	0.03	0.0075	0.0060	0.486	0.508	1.0576	1.0447
Ti6	0.06	0.0150	0.023	0.472	0.505	1.1186	1.0667
Ti10	0.10	0.0250	0.0280	0.469	0.502	1.1301	1.0664

$X_{gel} = x/4$; X_s = Ti/(Ti+Al+P), Y_s = Al/(Ti+Al+P), Z_s = P/(Ti+Al+P) in the solid.

The temperature range of TGA measurements was from 25 °C up to 1000 °C, using a heating rate of 10 °C.min^{-1}.

3. Results and Discussion

Figure 3 presents the pH of the reaction mixture as a function of the crystallization time. It can be observed that the gel pH increases with crystallization time up to a maximum value of around 7. This can be explained through the consumption of phosphoric acid by pseudoboehmite (an insoluble hydroxide) during the crystallization. Exception to samples mixture Ti10T*y*, there was a tendency of decreasing of the pH of reaction mixture as the Titanium contents increases. This tendency could be a consequence of the fact that the Titanium source is an acid (hexafluorotitanic).

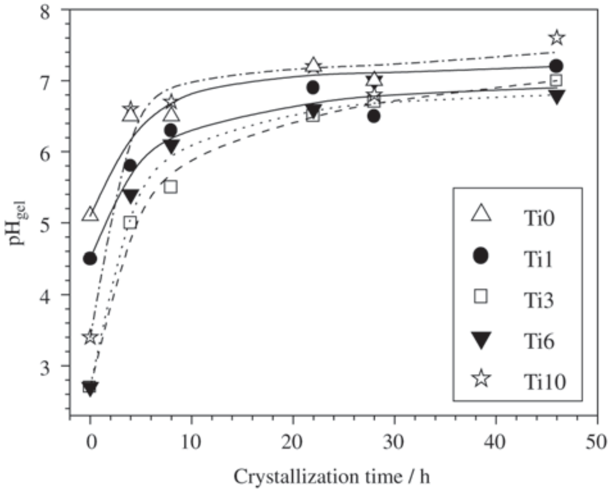

Figure 3. pH of the reaction mixture containing different Ti contents as a function of the crystallization time.

Figure 4 illustrates the crystallinity of the TAPO-5 samples as a function of the crystallization time. It can be observed that the crystallinity increases rapidly in the first hours and reaches a level value, which increases as the Titanium content is higher up to $x = 0.06$. This increasing in crystallinity, as the isomorphic substitution increases, was also observed during the incorporation of other elements in AlPOs as Mg[11] or Co[12]. However, as observed during the incorporation of these two elements, also in the case of Titanium there is a limit for the crystallinity and the maximum value for $x = 0.10$ was lower than that of $x = 0.06$.

Figure 5 shows the X-ray patterns of several titanium-substituted AFI samples, prepared with 46 h of crystallization. The patterns are very similar to that reported[4], indicating that there aren't other phases, except the sample Ti3, which presented some tridimite as contaminant. It was reported[13] that, when the pH during the synthesis of crystalline aluminophosphates is below 3.0, it could origin dense phases and when the pH is above 10.0 it could dissolve the product or precipitate some metal hydroxides. This could be the reason for the contamination, since TAPO-5 samples synthesized with $x = 0.03$ and 0.06 presented an initial pH below 3.0. However, only Ti3 (TAPO-5, $x = 0.03$) exhibited tridimite as contaminant phase.

The Table 1 presents the chemical analysis of TAPO-5 samples synthesized with 46 h and compares them with the gel composition.

This Table 1 illustrates that the Ti and P molar fraction in the solid is higher than in the gel. This indicates that

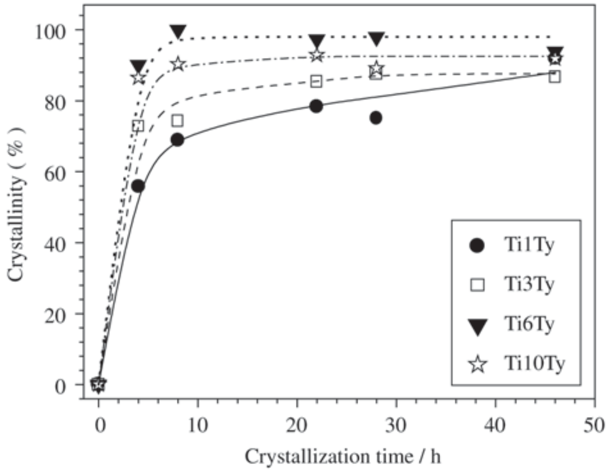

Figure 4. Crystallinity of the TAPO-5 samples as a function of the crystallization time.

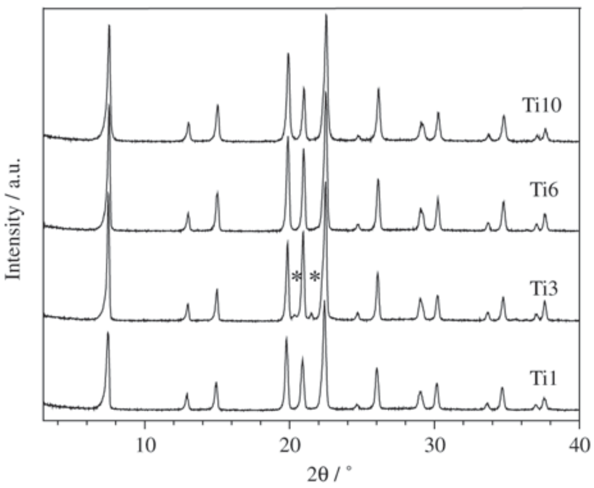

Figure 5. X-ray patterns of TAPO-5, with 46 h of crystallization. *tridimite phase.

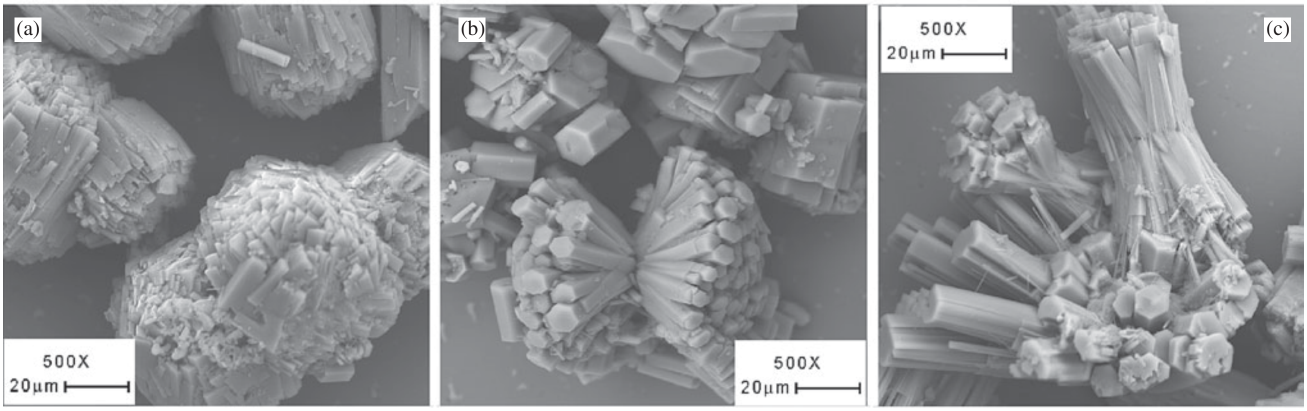

Figure 6. Micrographs of TAPO-5, with 46 h crystallization (*a*) Ti1, (*b*) Ti3 and (*c*)Ti10.

Table 2: DRS-UV bands of TAPO-5.

	UV (200-400 nm)		
	FT[a]	FO[b]	A[c]
Ti0	210	250	absent
Ti1	211	259	312
Ti3	212	258	293
Ti6	211	263	308
Ti10	211	258	298

Ti sites: [a] framework tetrahedral; [b] framework octahedral; [c] anatase.

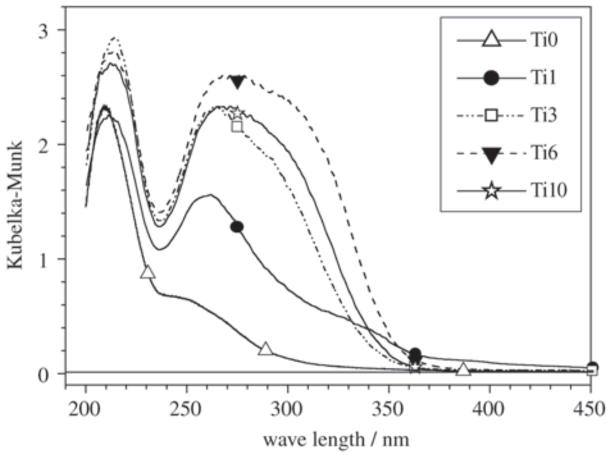

Figure 7. DRS-UV from TAPO-5, with 46 h of crystallization and different Ti contents.

aluminum forms soluble complexes in the presence of the template.

Figure 6 shows micrographs of TAPO-5 samples synthesized with different Ti contents and 46 h crystallization. It can be observed that the particles of the material are formed by aggregates, and the morphologies changes as the Ti contents in the reaction mixture increases. The aggregates obtained from the mixtures with the lower Ti content are compact and have a external rounded shape[4], while the one formed from mixture with higher Ti are formed by hexagonal needles-like crystals[6,9].

Figure 7 and Table 2 present the DRS-UV results from TAPO-5. The signal at 211 nm is attributed to Ti (IV) species in framework tetrahedral positions. The origin of the signal at around 261 nm is not yet well established. Some authors[4] suggest they are originated by the presence of octahedral framework Ti, others[8] to the presence of extraframework TiO_2 species (di- and trimers). One of the principal phases, which contaminate Ti-molecular sieves, is TiO_2 in the form of anatase[4] whose UV signal appears around 320 nm. The samples of TAPO-5 synthesized in this work showed a 3rd signal in the region of about 300 nm, which could be assigned to this phase. AlPO-5, that means, the sample that has no Ti its composition (Ti0, $x = 0.0$), has also signals in the UV region, at about 210 and 250 nm. Zanjanchi and Rashidi[14] attributed these signals to charge transfer from O → Al and to the presence of template occluded in the channels of the AFI framework. So, in the spectra of samples containing Ti, besides the signals involving this element, there are also these two contributions.

Figure 8 shows the thermograms of TAPO-5 (and the derivatives) measured under oxidant (Figs. 8a and 8b) and inert (Figs. 8c and 8d) ambient.

The thermograms measured under oxidant atmosphere present four temperature ranges (*A, B, C* and *D*) associated to different weight loss processes. The first range *A* ($T < 150$ °C) is attributed to water loss. The range *B*

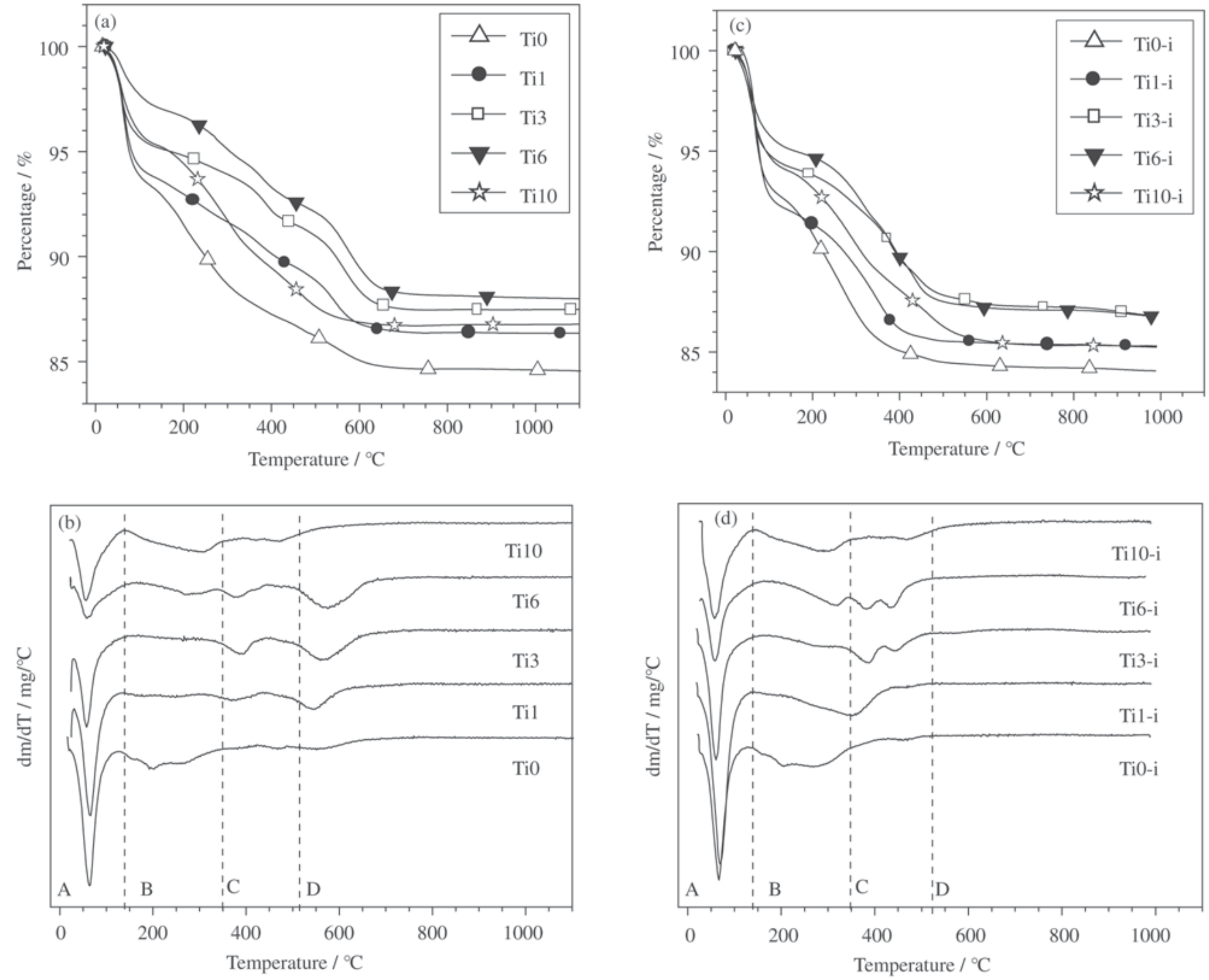

Figure 8. Thermograms of TAPO-5 in oxidant atmosphere: a) TGA, b) corresponding DTG; and inert atmosphere: c) TGA, d) corresponding DTG.

(150 < T < 320 °C) is associated to desorption of the physically occluded template or decomposition of alkylammonium phosphates[11]. The range *C* (320 < T < 520 °C) is ascribed to the decomposition of protonated template, which is compensation cation of the charge originated by the isomorphic substitution of framework $[PO_4^+]$ by $[TiO_4]$. The temperature range *D* (T > 520 °C) is attributed to coke oxidation, formed from decomposition of protonated template. This attribution is confirmed by the absence of this weight loss in the thermograms obtained under inert atmosphere. The weight loss in the temperature ranges *A, B*, and *C* were also found in the thermograms obtained under inert atmosphere and the attributions are the same of that measured under oxidant atmosphere.

4. Conclusions

Using various characterization techniques, it was possible to observe the influence of Ti content on the properties of microporous crystalline aluminophosphates with AFI structure, synthesized using a new Ti source (hexafluorotitanic acid). The XRD showed that the product obtained using this Ti source was not very different from the product using the organic sources. However, DRS-UV showed that using hexafluorotitanic acid there was formation of anatase at lower Ti content, compared when to Ti-organic sources are used. The thermogravimetry showed the presence of protonated template in the samples containing Ti, which compensates the negative charges in the AFI framework, formed as a consequence of the isomorphic substitution of $[PO_4^+]$ by $[TiO_4]$.

Acknowledgements

We acknowledge to CAPES and PRONEX/CNPq for financial assistance, to 'Laboratório de Caracterização Eletrônica' (LCE) for the use of the SEM and to 'Laboratório Interdisciplinar de Eletroquímica e Cerâmica' (LIEC) for the use of the DRS-UV equipment.

References

1. Bialek, R.; Meier, W.M.; Davis, M.; Annen, M.J. *Zeolites*, v. 11, p. 438, 1991.
2. Taramasso, M.; Perego, G.; Notari, B. U.S. Patent, 4,410,501, 1983.
3. Ulagappan, N.; Krishnasamy, V.K. *J. Chem. Society: Chem. Communication*, p. 373, 1995.
4. Ulagappan, N.; Krishnasamy,V. *Indian J. of Chemistry*, 35A, p. 920, 1996.
5. Prakash, A.M.; Kurshev, V.; Kevan, L. *J. Phys. Chemistry B.*, n. 101, p. 9794, 1997.
6. Akolekar, D.B.; Ryoo, R. *J. Chem. Society: Farad. Trans.*, n. 92 (22), p. 4617, 1996.
7. Zahedi-Niaki, M.H.; Zaidi, S.M.J.; Kaliaguine, S. *Microporous and Mesoporous Materials*, n. 32, p. 251, 1999.
8. Zahedi-Niaki, M.; Kapoor, M.; Kaliaguine, S. *J. of Catalysis*, n. 177, p. 231, 1998.
9. Zahedi-Niaki, M.H.; Joshi, P.N.; Kaliaguine, S. Progress in Zeolite and Microporous Materials. Studies in Surface Science and Catalysis, Elsevier Science B. V., v. 105, p. 1013, 1997.
10. Schoonheydt, R.A. in Characterization of Heterogeneous Catalysts - Chemical Industries , v. 15. Edited by Francis Delannay, p. 125-160, 1984.
11. Rios, S.P.O; Giotto, M.V.; Cardoso, D. 10° Congresso Brasileiro de Catálise, v. 2, p. 392, 1999.
12. Shiralkar, V.P.; Saldarriaga, C.H.; Perez, J.O.; Clearfield, A.; Chen, M.; Anthony, R.G.; Donohue, J.A. *Zeolites*, v. 9, p. 474, 1989.
13. Wilson, S.T. Introduction to Zeolite Science and Practice Elsevier Science Publishers B. V. Amsterdam, p.137, 1991.
14. Zanjanchi, M.A.; Rashidi, M.K. *Spectrochimica Acta* Part A, n. 55, p. 947, 1999.